

# Spatial and temporal feedback control of traveling wave solutions of the two-dimensional complex Ginzburg–Landau equation.

Claire M. Postlethwaite and Mary Silber

*Department of Engineering Sciences and Applied Mathematics  
Northwestern University  
Evanston, IL 60208 USA*

---

## Abstract

Previous work has shown that Benjamin–Feir unstable traveling waves of the complex Ginzburg–Landau equation (CGLE) in two spatial dimensions cannot be stabilized using a particular time-delayed feedback control mechanism known as ‘time-delay autosynchronisation’. In this paper, we show that the addition of similar *spatial* feedback terms can be used to stabilize such waves. This type of feedback is a generalization of the time-delay method of Pyragas (*Phys. Letts. A* **170**, 1992) and has been previously used to stabilize waves in the one-dimensional CGLE by Montgomery and Silber (*Nonlinearity* **17**, 2004). We consider two cases in which the feedback contains either one or two spatial terms. We focus on how the spatial terms may be chosen to select the direction of travel of the plane waves. Numerical linear stability calculations demonstrate the results of our analysis.

---

## 1 Introduction

During the past two decades considerable progress has been made in our understanding of the spontaneous emergence of patterns in spatially-extended non-equilibrium systems. The existence of simple spatial or spatio-temporal patterns has been rigorously established on the basis of equivariant bifurcation theory (see [1] and references therein). However, these simple patterns are often unstable in a given system, which evolves instead to a state of spatio-temporal chaos. Patterns that result from a symmetry-breaking Hopf bifurcation seem to be especially vulnerable to instability. A current challenge in pattern-formation research is to develop control schemes that stabilize the simple patterned states, so that a desired, otherwise unstable, solution may

be realized. This paper extends current research on feedback control of oscillatory patterns, focusing on traveling wave solutions of the two-dimensional complex Ginzburg–Landau equation. One of the goals of this line of research is to develop control algorithms that exploit the underlying symmetries of a targeted pattern in order to stabilize it in a non-invasive fashion. That is, if the pattern is invariant under some spatial, temporal or spatio-temporal transformation, then it may be possible to construct a feedback based on this transformation which vanishes when the target pattern is achieved. For example, if the pattern has the property that  $A(\mathbf{x}, t) = A(R\mathbf{x}, t - \tau)$  where  $R\mathbf{x}$  is some Euclidean transformation of the spatial variable, and  $\tau \geq 0$  is a possible time delay, then a feedback which is proportional to  $A(R\mathbf{x}, t - \tau) - A(\mathbf{x}, t)$  will be non-invasive.

Ott, Grebogi and Yorke [2] were the first to develop a control algorithm that suppresses chaos in favor of a simple unstable periodic orbit (UPO) in low-degree-of-freedom chaotic systems. In this approach, small perturbations are applied to a system parameter in order to keep the system close to the UPO. However, this method requires constant monitoring of the system, and also may not be effective in rapidly evolving systems.

Pyragas [3] introduced a second approach, sometimes called ‘time-delayed autosynchronisation’ (TDAS), in which the feedback is proportional to the difference between the current and a past state of the system. That is, the feedback is  $F = \gamma(A(t) - A(t - \Delta t))$  where  $\Delta t$  is the period of the desired UPO, and  $A(t)$  is some state variable. This method has a number of attractive properties. First, the UPO of the original system will also be a solution of the system with feedback, and so control may be achieved in a non-invasive manner. Second, the only information required a priori is the period of the desired UPO. The method has been implemented successfully in a variety of laboratory experiments on electronic [4,5], laser [6], plasma [7,8,9], mechanical [10] and chemical systems [11,12,13,14]; more examples can be found in a recent review by Pyragas [15].

An extension of TDAS proposed by Socolar et al. [16] incorporates information at many previous times and is known as ‘extended time-delayed autosynchronisation’ (ETDAS). This method was used by Bleich and Socolar [17] to stabilize unstable traveling wave solutions of the complex Ginzburg–Landau equation (CGLE) in one spatial dimension. For spatially-extended pattern-forming systems, other proposed modifications of the time-delay autosynchronization scheme of Pyragas include *global* feedback control [18,19,20], where the magnitude of the feedback depends on some spatial average, or maximum, of a quantity at an earlier time. Yet others take into account the spatial periodicity, as well as temporal periodicity, of the targeted pattern. For instance, Lu, Yu and Harrison [22] used numerical simulations of the two-dimensional Maxwell–Bloch equations describing a three-level laser system to demonstrate

that spatio-temporal chaos could be suppressed by applying a linear combination of time-delay feedback and an analogous spatially-translated feedback term of the form:

$$F_s = \rho\{[E(x + x_0, y, t) - E(x, y, t)] + [E(x, y + y_0, t) - E(x, y, t)]\}.$$

Here  $\mathbf{d}_1 = (x_0, 0)$  and  $\mathbf{d}_2 = (0, y_0)$  are translation vectors associated with the feedback; the feedback is non-invasive when the resulting pattern is periodic in each of the  $\mathbf{d}_j$ -directions, with spatial periods  $|\mathbf{d}_j|$ . Their numerical investigations reveal that these two spatial controls somehow select the direction of travel of the stabilized plane wave. This type of feedback, with a combination of temporal and spatial terms, was extensively studied by Montgomery and Silber [21] in the context of the one-dimensional CGLE.

The aim of our paper is to extend the results of [21] to the CGLE in two spatial dimensions. This problem is interesting since Harrington and Socolar [23] have shown that unstable traveling waves in the 2D CGLE *cannot* be stabilized using only temporal feedback, due to the presence of torsion-free modes (that is, modes which have purely real Floquet multipliers). We circumvent this difficulty by using a combination of temporal and spatial terms, as in [21], and additionally consider the effect of having either one or two spatially shifted terms in order to steer the direction of the traveling waves in the plane.

Our analysis is based on a linear stability analysis of the traveling wave solutions of the CGLE. The analysis leads to a system of delay differential equations (see [24,25] for more on DDEs). We find stability boundaries by searching for critical curves/surfaces of Hopf bifurcations within the system of DDEs. The analysis is made possible because the CGLE admits an exact family of solutions in the form of a traveling plane waves  $Re^{i\mathbf{k}\cdot\mathbf{x}+i\omega t}$ , parameterized by the wave vector  $\mathbf{k}$ . For this problem the dispersion relation that relates  $|\mathbf{k}|$  and  $\omega$  is known precisely.

We expect that our methods could equally well be applied to other spatially extended systems for which traveling plane waves exist. Such solutions arise for instance when a spatially-uniform solution undergoes a Hopf bifurcation. However, in many instances, the form of the wave and the dispersion relation are unknown, or known only approximately. In this case, we propose that just one spatial term be incorporated in the feedback, and consider target waves that travel in a direction relative to this feedback term so that both the temporal and spatial feedback terms vanish. In this way the wavenumber and frequency of the plane wave can be matched even when the dispersion relation is unknown, although the direction of travel must be left free.

This paper is organized as follows. In Section 2 we review some properties of the CGLE and the feedback we are applying, and in Section 3 we describe previously known results regarding these systems. In Section 4 we discuss

the effects of additional spatial feedback and how the spatial shifts must be chosen in order to stabilize the wave. Section 5 contains a geometric way to think about the results of [21] and in Section 6 we provide a numerical example to demonstrate our results. Section 7 concludes.

## 2 Problem setup

### 2.1 The complex Ginzburg–Landau equation

In this section we review some properties of traveling wave solutions of the complex Ginzburg–Landau equation (CGLE). The CGLE is an amplitude equation for some disturbance  $A(\mathbf{x}, t)$  in a spatially extended system near the onset of a Hopf bifurcation that sets in with zero wavenumber, *i.e.* a spatially–uniform oscillatory instability. After appropriate rescalings and in a frame that is oscillating at the Hopf frequency, it can be written generically as:

$$\frac{\partial A}{\partial t} = A + (1 + ib_1)\nabla^2 A - (b_3 - i)|A|^2 A, \quad (1)$$

where  $b_1$  and  $b_3$  are real parameters. We consider only the situation just after a supercritical Hopf bifurcation, so the coefficient of the linear term is positive (and has been rescaled to equal unity) and the parameter  $b_3$  is assumed to be positive. In this paper, we consider the spatial extent of the problem to be two-dimensional, so  $\mathbf{x} = (x, y)$ . We consider traveling wave solutions of the form

$$A_{\text{TW}} = R e^{i\mathbf{k}\cdot\mathbf{x} + i\omega t}, \quad (2)$$

where the amplitude  $R$  and frequency  $\omega$  are determined by the wavenumber  $k = |\mathbf{k}|$  through the relations

$$R^2 = \frac{1 - k^2}{b_3}, \quad \omega = R^2 - b_1 k^2. \quad (3)$$

Since  $b_3 > 0$  it follows from (3) that  $k < 1$ . We also assume that  $\mathbf{k} \neq \mathbf{0}$ .

In the Benjamin–Feir unstable regime ( $b_1 > b_3 > 0$ ) all solutions of the form (2) are unstable. In this paper we investigate how the addition of feedback terms to (1) affects the linear stability of these solutions in this regime. Specifically we consider

$$\frac{\partial A}{\partial t} = A + (1 + ib_1)\nabla^2 A - (b_3 - i)|A|^2 A + F, \quad (4)$$

where  $F$  is a feedback term given by

$$F = \gamma[A(\mathbf{x}, t) - A(\mathbf{x}, t - \Delta t)] + \sum_{j=1}^N \rho_j [A(\mathbf{x} + \Delta \mathbf{x}_j, t) - A(\mathbf{x}, t)]. \quad (5)$$

The delay parameter  $\Delta t$  is positive, and we restrict our analysis to the case where  $\gamma$  (the gain) and  $\rho_j$  are real. We consider the two cases  $N = 1$  and  $N = 2$ , that is, the feedback  $F$  can contain either one or two spatially-shifted feedback terms.

In this paper, we study the stability of traveling waves for which the feedback terms vanish. We choose the spatial and temporal shifts  $\Delta \mathbf{x}_j$  and  $\Delta t$  such that

$$\Delta t |\omega| = 2\pi \quad \Delta \mathbf{x}_j \cdot \mathbf{k} = 2\pi n_j, \quad n_j \in \mathbb{Z}, \quad j = 1, \dots, N \quad (6)$$

for a specific targeted traveling wave of the form (2), with wavevector  $\mathbf{k} = (k_x, k_y)$  and frequency  $\omega$ .

There may be many other solutions to (4) for which the feedback term does not vanish. We do not study these solutions in this paper - our analysis is a purely local stability analysis assuming we are already close to the targeted wave.

Since we know the dispersion relation (3) relating the wave frequency  $\omega$  and the wavenumber  $k = |\mathbf{k}|$ , the spatial and temporal shifts are related and cannot be chosen independently. We now consider how the shifts must be chosen in the two cases  $N = 2$  and  $N = 1$ .

Note that if we were to choose  $N > 2$ , there would be some relations between the  $\Delta \mathbf{x}_j$  in order that they satisfy (6). For instance, for  $N = 3$ , we would need  $\Delta \mathbf{x}_3 = n_1 \Delta \mathbf{x}_1 + n_2 \Delta \mathbf{x}_2$  for some integers  $n_1$  and  $n_2$ . This is because we are in two spatial dimensions. We do not consider the cases of higher  $N$  here, but it may be that using additional shifted terms can increase the region of stability of the traveling waves, much in the same way as ETDAS [17].

For  $N = 2$ , we insist that  $\Delta \mathbf{x}_1$  and  $\Delta \mathbf{x}_2$  are not parallel ( $\Delta \mathbf{x}_1 \times \Delta \mathbf{x}_2 \neq 0$ ). Then for specified  $\Delta \mathbf{x}_1$  and  $\Delta \mathbf{x}_2$  there is a two-dimensional dual lattice of possible target wavevectors  $\mathbf{k}$ . The lattice generators  $\mathbf{k}_1$  and  $\mathbf{k}_2$  satisfy

$$|\mathbf{k}_j| = \frac{2\pi |\Delta \mathbf{x}_j|}{|\Delta \mathbf{x}_1 \times \Delta \mathbf{x}_2|}, \quad \mathbf{k}_j \cdot \Delta \mathbf{x}_j = 0, \quad j = 1, 2. \quad (7)$$

The frequency of the desired wave is specified by the choice of  $\Delta t$ , which must be consistent with the choice of  $\mathbf{k}$ , since the frequency and wavenumber are related *a priori* by the dispersion relation (3). (This ‘overspecification’ of the targeted wave is analogous to the one-dimensional case of [21], where one

temporal and one spatial term select  $\omega$  and  $k$  which are already related by the dispersion relation.) Note that if  $\mathbf{k}$  lies on the lattice, so also does  $-\mathbf{k}$ , and thus the direction (right/left) of travel of the wave is not selected.

If the same procedure were repeated for a different amplitude equation for which the dispersion relation were not known, then in the ‘overspecified’  $N = 2$  case there could be a discrepancy between the temporal and spatial feedback terms, and it may not be possible for both to vanish. However, in the case  $N = 1$ , there is more freedom, as we explain below.

For  $N = 1$  it is not possible to choose  $\Delta\mathbf{x}_1$  such that the spatially-shifted term targets a single traveling wave. That is, for a given  $n_1$ , there is a continuum of wavevectors  $\mathbf{k}$  for which  $\mathbf{k} \cdot \Delta\mathbf{x}_1 = 2\pi n_1$  and the spatial feedback term vanishes. The possible target  $\mathbf{k}$  for a given  $\Delta\mathbf{x}_1$  are indicated by the bold lines in Figure 1, in section 4. However, the choice of  $\Delta t$  selects some  $\omega$ , and hence  $|\mathbf{k}|$  is also selected, by the dispersion relation. The direction of  $\mathbf{k}$  (again, up to a sign) is selected by the spatially shifted term, and so a single traveling wave can be targeted. This is explained in more detail in Section 4.2.1.

Note that  $F$  can only improve the stability of the traveling waves if  $\gamma < 0$  and likewise  $\rho_j > 0$ . The reasons for this are explained in detail in [21] and we will only consider this parameter regime.

## 2.2 Stability analysis

The linear stability of traveling waves (2) is calculated by considering the effect of small amplitude perturbations, for some perturbation wavevector  $\mathbf{q} = (q_x, q_y)$ . We write

$$A = R e^{i\mathbf{k}\cdot\mathbf{x}+i\omega t} (1 + a_+(t) e^{i\mathbf{q}\cdot\mathbf{x}} + a_-(t) e^{-i\mathbf{q}\cdot\mathbf{x}}), \quad (8)$$

substitute into (4) and linearize in  $a_+$  and  $a_-$ . This results in a system of delay differential equations for  $a_+$  and the complex conjugate of  $a_-$  (denoted by  $a_-^*$ ):

$$\frac{d}{dt} \begin{pmatrix} a_+(t) \\ a_-^*(t) \end{pmatrix} = J \begin{pmatrix} a_+(t) \\ a_-^*(t) \end{pmatrix} + \gamma \left[ \begin{pmatrix} a_+(t) \\ a_-^*(t) \end{pmatrix} - \begin{pmatrix} a_+(t - \Delta t) \\ a_-^*(t - \Delta t) \end{pmatrix} \right], \quad (9)$$

where

$$J = \begin{pmatrix} -c_1 q^2 - c_2 R^2 & -c_2 R^2 \\ -c_2^* R^2 & -c_1^* q^2 - c_2^* R^2 \end{pmatrix} + 2\mathbf{k}\cdot\mathbf{q} \begin{pmatrix} -c_1 & 0 \\ 0 & c_1^* \end{pmatrix} + \sum_{i=1}^N \rho_j (e^{i\mathbf{q}\cdot\Delta\mathbf{x}_j} - 1) \begin{pmatrix} 1 & 0 \\ 0 & 1 \end{pmatrix} \quad (10)$$

with  $c_1 = 1 + ib_1$ ,  $c_2 = -i + b_3$  and  $q = |\mathbf{q}|$ .

In the following sections we review previous results concerning feedback control in equations similar to (9) and then present our new results.

### 3 Previous results

Our stability analysis builds on results of Harrington and Socolar [23], Nakajima [26] and Montgomery and Silber [21]. For completeness, in this section we give a summary of the results of [23] and [26], and also of previously known results concerning some instabilities of the CGLE without feedback. We discuss details of [21] in Section 5.

#### 3.1 Instabilities with no feedback terms

In the absence of any feedback terms (i.e.  $\gamma = \rho_j = 0$ ), traveling waves are stable to perturbations with wavevector  $\mathbf{q}$  if both eigenvalues of the Jacobian (10) have negative real part.

The Benjamin–Feir (B–F) instability is a long wavelength instability, that is, perturbations with  $q = |\mathbf{q}|$  sufficiently small will grow. In the limit  $q \ll 1$ , a simple calculation shows that one eigenvalue of  $J$  always has negative real part, and the other has real part equal to:

$$\left(\frac{b_1}{b_3} - 1\right) q^2 + \frac{2}{b_3 R^2} \left(1 + \frac{1}{b_3^2}\right) (\mathbf{k} \cdot \mathbf{q})^2 + O(q^3).$$

Hence, if  $b_1 > b_3 > 0$  (the B–F unstable regime), then this is positive for all  $\mathbf{k}$ , and long wavelength perturbations will grow.

A second type of instability important to our subsequent analysis, is associated with perturbations with  $\mathbf{k} \cdot \mathbf{q} = 0$  ( $q$  no longer necessarily small). It can be shown [23] that these perturbations grow for small enough  $q$ , that is, those with

$$q^2 < q_{\text{cr}}^2 = \frac{2R^2(b_1 - b_3)}{1 + b_1^2}. \quad (11)$$

Perturbations with  $\mathbf{k} \cdot \mathbf{q} = 0$  and  $q > q_{\text{cr}}$  decay.

When  $q$  is sufficiently large, the eigenvalues of  $J \sim -q^2$ , so all sufficiently shortwave perturbations will decay. However, there may be other regions of unstable  $\mathbf{q}$  in addition to those described above.

### 3.2 A result of Harrington and Socolar

We now summarize a result from Harrington and Socolar [23] concerning the stabilization of plane waves in the 2D CGLE with only temporal feedback. Their result relies on a proof of Nakajima [26] which has recently [27,28] been shown to be incorrect. However, as we discuss below, the result of Nakajima does still hold in some cases, and the results of [23] are still correct.

The claim of Nakajima is as follows. Suppose an ODE

$$\dot{x} = f(x(t), t), \quad x \in \mathbb{R}^n, \quad (12)$$

contains an unstable periodic orbit,  $x^*(t)$ , with period  $T$ . Feedback is added to (12) so it is now of the form

$$\dot{x}(t) = f(x(t), t) + K(x(t) - x(t - T)), \quad (13)$$

where  $K$  is an  $n \times n$  gain matrix. Then if the linearization of (12) about the orbit  $x^*(t)$  has an odd number of positive, real unstable Floquet multipliers then there is no value of  $K$  for which  $x^*(t)$  is a stable solution of (13).

The flaw in the proof of Nakajima is that the neutral Floquet multiplier associated with perturbations in the direction of the periodic orbit was neglected.

However, in both the example of Harrington and Socolar, and in our work, the analysis of the stability of the traveling wave has been reduced to the study of the stability of a fixed point (namely, the zero solution to the linear DDE (9)). The result of Nakajima *can* be applied to hyperbolic fixed points, since they do not have a trivial Floquet multiplier, and so the results of [23] still stand. (A similar result for fixed points in maps, rather than flows, is given by Ushio [29].) In our examples, the perturbation along the periodic orbit which yields a neutral Floquet multiplier is associated with a perturbation with wavevector  $\mathbf{q} = \mathbf{0}$ . It is not this type of perturbation we are concerned with in the following.

The result of Harrington and Socolar is summarized as follows. Consider (9) with no spatial feedback, that is,  $\rho_j = 0$ . In 2D there always exists an unstable perturbation wavenumber  $\mathbf{q}$  which satisfies  $\mathbf{k} \cdot \mathbf{q} = 0$ . In this situation, the Jacobian  $J$  is equal to

$$\begin{pmatrix} -c_1 q^2 - c_2 R^2 & -c_2 R^2 \\ -c_2^* R^2 & -c_1^* q^2 - c_2^* R^2 \end{pmatrix}$$

where  $\text{Re}(c_1), \text{Re}(c_2) > 0$ . If  $0 < q < q_{cr}$ , then  $J$  has real trace and real, negative determinant, hence has real eigenvalues of opposite sign.



Note that in only one spatial dimension, we can only have  $\mathbf{k} \cdot \mathbf{q} = \mathbf{0}$  if either  $\mathbf{q} = \mathbf{0}$  or  $\mathbf{k} = \mathbf{0}$ , so the same result does not apply. The ‘flat’ perturbations with  $\mathbf{q} = \mathbf{0}$  do not cause instabilities for  $\gamma \leq 0$ , which is the parameter range we are interested in.

## 4 Additional spatial feedback

In this section we extend the results described above to include the effects of additional spatial feedback, with either one or two spatial terms. This section is organized as follows. First, we show that there are some perturbation wavevectors  $\mathbf{q}$  which are unaffected by the spatial feedback. We then discuss how the displacements  $\Delta\mathbf{x}_j$  must be chosen to target a particular wavevector  $\mathbf{k}$ , for both the cases  $N = 1$  and  $N = 2$ .

### 4.1 Perturbations unaffected by spatial feedback

Consider the Jacobian matrix  $J$  given in (10). If the perturbation wavevector  $\mathbf{q}$  satisfies  $\mathbf{q} \cdot \Delta\mathbf{x}_j = 2\pi m_j$ , for some  $m_j \in \mathbb{Z}$ , then  $J$  is the same as if  $\rho_j = 0$ . Hence, these perturbations  $\mathbf{q}$  are not affected by the spatial feedback. Combining this with the results of Harrington and Socolar [23] described in the previous section, if these  $\mathbf{q}$  are unstable for the system with no feedback, and additionally satisfy  $\mathbf{k} \cdot \mathbf{q} = 0$ , then the traveling waves cannot be stabilized for any values of  $\rho_j$  and  $\gamma$ . That is, if there is a  $\mathbf{q} \neq \mathbf{0}$  which satisfies

$$\mathbf{k} \cdot \mathbf{q} = 0, \quad \mathbf{q} \cdot \Delta\mathbf{x}_j = 2\pi n_j, \quad n_j \in \mathbb{Z} \quad \text{and} \quad |\mathbf{q}| < q_{cr}, \quad (14)$$

then the traveling waves cannot be stabilized.

If there are no such  $\mathbf{q}$ , then it is possible that there exists some choice of  $\rho_j$  and  $\gamma$  for which the traveling wave is stable.

### 4.2 Choice of $\Delta\mathbf{x}_j$

Recall that in order for the spatial feedback to vanish at the targeted wave solution, we require that

$$\mathbf{k} \cdot \Delta\mathbf{x}_j = 2\pi n_j, \quad n_j \in \mathbb{Z}. \quad (15)$$

In one spatial dimension, this gives a unique choice of  $\Delta\mathbf{x}_j$  (for say,  $n_j = 1$ ) for a given  $\mathbf{k}$ , but in two spatial dimensions this is not the case. We now discuss this further.

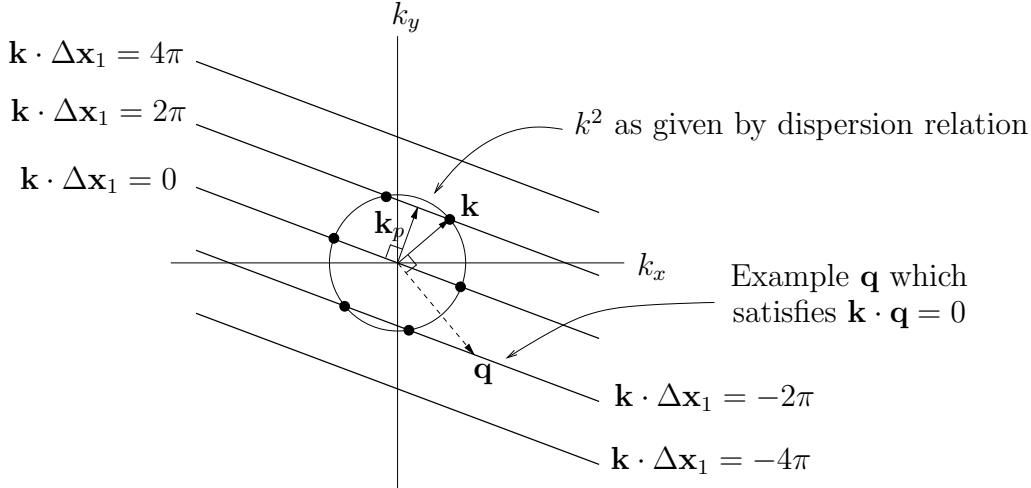


Fig. 1. The bold lines indicate those points in  $\mathbf{k}$ -space which satisfy  $\mathbf{k} \cdot \Delta \mathbf{x}_1 = 2\pi n_1$  ( $n_1 \in \mathbb{Z}$ ). The vector  $\mathbf{k}_p$  is parallel to  $\Delta \mathbf{x}_1$ . The circle indicates the wavevectors  $\mathbf{k}$  for which the temporal feedback term vanishes with  $|\omega| \Delta t = 2\pi$ . The intersections of the circle and the lines (marked by dots) are the possible target  $\mathbf{k}$ . As the direction of  $\mathbf{k}$  gets closer to  $\mathbf{k}_p$ , either by changing the size of the circle, or altering the angle of  $\Delta \mathbf{x}_1$ , the magnitude of the  $\mathbf{q}$  which satisfy  $\mathbf{k} \cdot \mathbf{q} = 0$  and also lie on the bold lines increases.

#### 4.2.1 The case $N = 1$

For  $N = 1$  there is a continuum of wavevectors  $\mathbf{k}$  for which  $\mathbf{k} \cdot \Delta \mathbf{x}_1 = 2\pi n_1$  and the feedback term vanishes. The possible  $\mathbf{k}$  are indicated by the bold straight lines in Figure 1. However, isolated  $\mathbf{k}$  can be picked out from this continuum by the temporal feedback term (which fixes  $\Delta t$  and hence  $\omega$ ) and the dispersion relation. The dispersion relation fixes  $k^2$  for a given  $\omega$  and so gives a circle of possible wavevectors. If we let  $|\omega| \Delta t = 2\pi n$  for some integer  $n > 1$ , then this will give a family of circles, of decreasing  $k$  as  $n$  increases (since  $k$  must decrease as  $\omega$  increases), however, we only consider  $n = 1$ . The intersection of this circle and the straight lines in Figure 1 give the possible  $\mathbf{k}$  for which the feedback term vanishes. In this example, there are three possible  $\mathbf{k}$  (up to a sign). As we explain below, the  $\mathbf{k}$  with direction closest to that of  $\Delta \mathbf{x}_1$  will be the easiest to stabilize. However, it is certainly possible that more than one of these  $\mathbf{k}$  may be simultaneously stabilized.

If the dispersion relation for a system is known, as is the case for the CGLE, then the location of this circle is known, and  $\Delta t$  and  $\Delta \mathbf{x}_1$  can be chosen to target a particular traveling wave. If the dispersion relation is not known, then the location of the circle is not known, but it still exists. In this case, we can, say, choose  $\Delta t$  to pick the frequency of the target wave, and also pick some  $\Delta \mathbf{x}_1$ . We will not be able to choose in advance the wavevector  $\mathbf{k}$  of the resulting targeted wave, but the possible  $\mathbf{k}$  for which the feedback vanishes will be isolated in  $\mathbf{k}$ -space. This method provides us with a possible mechanism for using this stabilization scheme for a system in which the dispersion relation is

not known.

If there is a  $\mathbf{q}$  which satisfies (14), it will also lie on the bold lines in Figure 1. However, for a given  $\mathbf{k}$ ,  $\Delta\mathbf{x}_1$  can be chosen in such a way that there are no  $\mathbf{q}$  which satisfy the resonance conditions (14). To see this, consider the situation where  $\Delta\mathbf{x}_1$  is chosen to be almost parallel to  $\mathbf{k}$ , then the only  $\mathbf{q}$  perpendicular to  $\mathbf{k}$  which also lie on the bold lines will have a very large magnitude and hence do not correspond to wavenumbers of destabilizing perturbations. Once  $\Delta\mathbf{x}_1$  is chosen to avoid the resonance conditions (14) the methods developed in [21] can then be used to determine the stability of the traveling waves.

By analogy with the one-dimensional case, we might hope that we are able to stabilize the wave for which  $\mathbf{k}$  and  $\Delta\mathbf{x}_1$  are parallel (indicated by  $\mathbf{k}_p$  on Figure 1). However, this is not the case since there always exist unstable longwave perturbations ( $q$  small) which satisfy  $\mathbf{k}_p \cdot \mathbf{q} = \mathbf{q} \cdot \Delta\mathbf{x}_1 = 0$ , and these perturbations are unaffected by the spatial feedback. Hence this plane wave cannot be stabilized in this fashion.

#### 4.2.2 The case $N = 2$

For the spatial feedback with two terms to vanish at the targeted wave solution,  $\mathbf{k}$  must satisfy

$$\mathbf{k} \cdot \Delta\mathbf{x}_1 = 2\pi n_1, \quad \mathbf{k} \cdot \Delta\mathbf{x}_2 = 2\pi n_2, \quad n_1, n_2 \in \mathbb{Z}.$$

This gives a lattice of possible target wavevectors with generators as given in equation (7). An example lattice is shown in Figure 2. Recall that for the CGLE we must have  $k = |\mathbf{k}| < 1$ , so for a given target  $\mathbf{k}$ , it is possible to choose  $\Delta\mathbf{x}_1$  and  $\Delta\mathbf{x}_2$  such that  $\mathbf{k}$  and  $-\mathbf{k}$  are the only non-trivial lattice points inside the unit circle. However, for a specific choice of  $\mathbf{k}$ , the choice of  $\Delta\mathbf{x}_1$  and  $\Delta\mathbf{x}_2$  resulting in an appropriate lattice is not unique.

The perturbations  $\mathbf{q}$  which satisfy (14) will lie on the same lattice as  $\mathbf{k}$ . If  $q_{cr}$  is small enough, there will be no unstable  $\mathbf{q}$  (that is, with  $|\mathbf{q}| < q_{cr}$ ) which lie on the lattice. Therefore, so long as  $\Delta\mathbf{x}_1$  and  $\Delta\mathbf{x}_2$  are chosen appropriately, the theorem of Nakajima does not apply. The methods developed in [21] can then be used to determine the regions of stability for these waves. In the next section we review the approach taken in [21].

## 5 Analysis

In this section we discuss a result found in Montgomery and Silber [21]. They show that for the CGLE in 1D with feedback as in (4), the ‘best’ choice of  $\gamma$  is

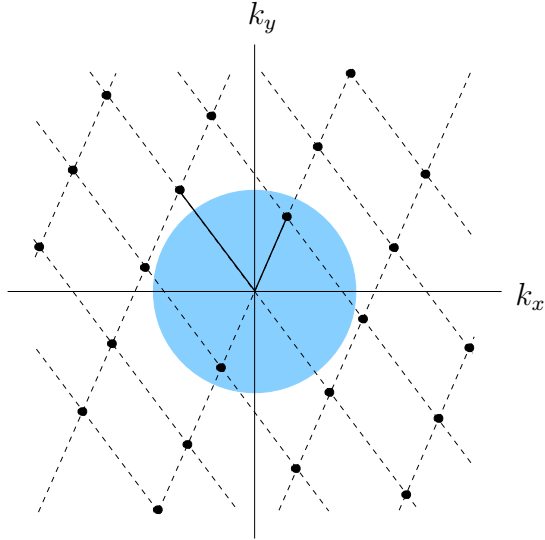


Fig. 2. The figure shows a lattice of possible  $\mathbf{k}$ -vectors for which the spatial feedback vanishes in the case  $N = 2$ . The bold lines indicate the lattice generators. The shaded region shows those  $\mathbf{k}$  with  $|\mathbf{k}| < 1$ . In this example only two non-trivial lattice points lie within this disc.

$-1/\Delta t$ . That is, if it is possible to stabilize a traveling wave for some choice of feedback parameters, this can certainly be achieved by choosing  $\gamma = -1/\Delta t$ .

The proof given in [21] can be extended to two dimensions. Here we omit those details and give a briefer, and more intuitive reason as to why their result holds, although it is not rigorous.

We first reduce the delay differential equation (9) to a single equation by diagonalizing the matrix  $J$  to give

$$\dot{a}(t) = \hat{m}_1 a(t) + \gamma(a(t) - a(t - \Delta t)) \quad (16)$$

$$\dot{b}(t) = \hat{m}_2 b(t) + \gamma(b(t) - b(t - \Delta t)) \quad (17)$$

where  $a$  and  $b$  are appropriate linear combinations of  $a_+$  and  $a_-^*$ , and

$$\hat{m}_k = m_k + \sum_{j=1}^2 \rho_j (e^{i\mathbf{q} \cdot \Delta \mathbf{x}_j} - 1), \quad k = 1, 2.$$

The  $m_k$  are the eigenvalues of the Jacobian (10) with no feedback (that is,  $\rho_j = \gamma = 0$ ), with  $\text{Re}(m_1) > \text{Re}(m_2)$ . As described in [21], the  $b$  equation does not affect the stability boundary since it is associated with the more stable eigenvalue. We therefore concentrate on the  $a$  equation, and write  $\hat{m}_1 = \alpha(\mathbf{q}) + i\beta(\mathbf{q})$ , where  $\alpha$  and  $\beta$  are real functions of  $\mathbf{q}$ . Hence,  $\alpha(\mathbf{q})$  is the largest real part of the eigenvalues of  $J$  when there is no temporal feedback. Since the feedback can only improve the stability of the traveling waves, instabilities are only possible when  $\alpha(\mathbf{q}) > 0$ .

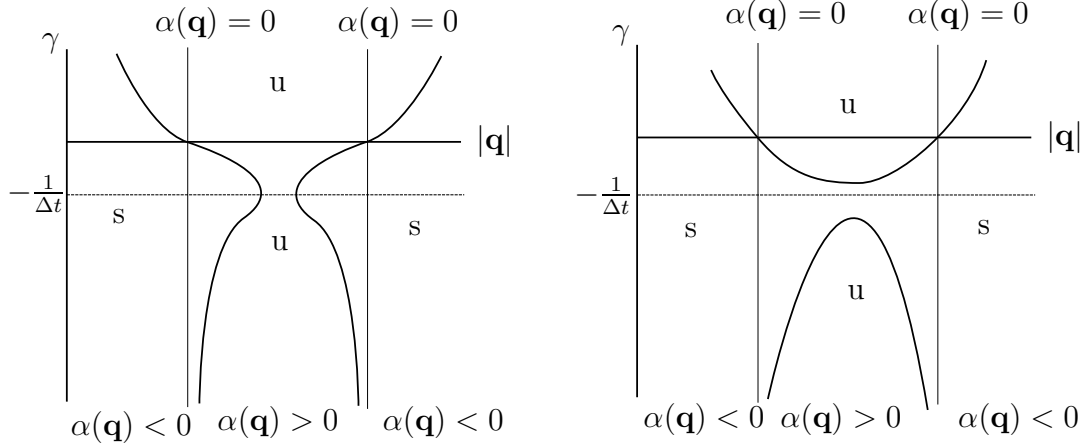


Fig. 3. Schematic diagram showing critical curves in unstable (left-hand picture) and stable (right-hand picture) cases. The transition between the two takes place at  $\gamma = -1/\Delta t$ . The regions of the diagram are marked as containing perturbations  $\mathbf{q}$  which are stable (s) or unstable (u).

Critical surfaces describing the boundaries between regions of stable and unstable perturbations have  $a(t) = e^{\lambda t}$  with  $\lambda = i\nu$ ,  $\nu \in \mathbb{R}$  (i.e. they are points of Hopf bifurcations since  $\nu \neq 0$ ). We can write equations for these surfaces in  $\gamma$ - $\mathbf{q}$  space, parameterized by  $\nu$ , as:

$$\alpha(\mathbf{q}) = \gamma(\cos \nu - 1) \quad (18)$$

$$\gamma \Delta t \sin \nu = \nu + \Delta t \beta(\mathbf{q}). \quad (19)$$

The results of [21] can be used to give an algebraic condition for the stability of the traveling waves. That is, if there are no solutions  $\nu$ ,  $\mathbf{q}$  to the equations

$$\cos \nu - 1 = -\Delta t \alpha(\mathbf{q}) \quad (20)$$

$$\sin \nu + \nu = -\Delta t \beta(\mathbf{q}) \quad (21)$$

then the traveling wave can be stabilized at  $\gamma = -1/\Delta t$ .

In Figure 3 we give a sketch of the shape of the curves given by (18) and (19) for a fixed direction of  $\mathbf{q}$ , in two cases, one before and one after a change of stability of the traveling waves. At points with  $\alpha(\mathbf{q}) = 0$ , the curves either intersect  $\gamma = 0$  (if  $\nu \neq 2\pi n$ ), or asymptote to  $\gamma = \pm\infty$  (when  $\nu = 2\pi n$ ).

These curves divide regions of stable and unstable perturbations. For a traveling wave to be stable, it must be stable for all perturbations  $\mathbf{q}$ . One mechanism by which the stability of a traveling wave can change is for two critical curves to collide at points with  $\frac{\partial \mathbf{q}}{\partial \gamma} = 0$ . Figure 3 shows a schematic of this transition. Of course, the stability of the wave could also hypothetically change without the two curves in the right hand picture of Figure 3 colliding; the minimum of the top curve would just have to extend below the maximum of the lower curve. We do not consider this mechanism of stability change here, but it is covered by the analysis in [21].

Hence, we wish to identify points on the critical curves which have  $\frac{\partial \mathbf{q}}{\partial \gamma} = 0$ , since it is at these points that the surfaces can collide and change the stability of the traveling waves. Differentiating (18) and (19) with respect to  $\gamma$ , and setting  $\frac{\partial \mathbf{q}}{\partial \gamma} = 0$  gives:

$$\gamma \sin \nu \frac{\partial \nu}{\partial \gamma} = \cos \nu - 1 \quad (22)$$

$$\Delta t \sin \nu = \frac{\partial \nu}{\partial \gamma} (1 - \gamma \Delta t \cos \nu) \quad (23)$$

Eliminating  $\frac{\partial \nu}{\partial \gamma}$  results in

$$(\cos \nu - 1)(1 + \gamma \Delta t) = 0.$$

When  $\cos \nu = 1$ , the critical curves asymptote to  $\gamma = \pm \infty$ ,  $\alpha(\mathbf{q}) = 0$ , so the only turning points with  $\frac{\partial \mathbf{q}}{\partial \gamma} = 0$  will be at  $\gamma = -\frac{1}{\Delta t}$ , which is the value identified as optimal in [21].

## 6 Numerical results

We now give two numerical examples to show that there are regions of parameter space in which traveling waves can be stabilized using the methods described above. The first example we give can be stabilized for  $N = 2$  but not, for the parameters we use, for  $N = 1$ . The second example can be stabilized for  $N = 1$ . We also demonstrate the way in which stability of the traveling wave is lost, as described above - two critical surfaces collide at  $\gamma = -1/\Delta t$ .

We used the Matlab package DDE-BIFTOOL [30] to analyze the linearized system (9) and search for Hopf bifurcations in order to locate the critical surfaces between stable and unstable perturbations in  $\gamma$ - $\mathbf{q}$  space. For our first example, the parameters used are  $b_1 = 2.5$ ,  $b_3 = 2$ . Without loss of generality, we choose  $\mathbf{k}$  to be parallel to the  $x$ -axis. The spatial shifts  $\Delta \mathbf{x}_1$  and  $\Delta \mathbf{x}_2$  are chosen to be parallel to the vector  $(1, 1)$  and  $\mathbf{k}$  respectively, and also to satisfy  $\Delta \mathbf{x}_j \cdot \mathbf{k} = 2\pi$ ,  $j = 1, 2$ . We choose  $\rho_1 = 0.01$  and  $\rho_2 = 0.007$ . Recall that the wave cannot be stabilized if there exist unstable perturbations with  $\mathbf{k} \cdot \mathbf{q} = 0$  and  $\mathbf{q} \cdot \Delta \mathbf{x}_j = 2\pi n_j$ . In this example,  $q_{cr} = \frac{2(1-k^2)}{29}$  and it is simple to check in each case that there are no such  $\mathbf{q}$  with  $|\mathbf{q}| < q_{cr}$ .

The contour plots of  $\alpha(\mathbf{q})$  in Figure 4 show the regions of  $\mathbf{q}$ -space in which it is possible to find instabilities - that is, those regions where  $\alpha(\mathbf{q}) > 0$ . Note that there is a symmetry  $\mathbf{q} \rightarrow -\mathbf{q}$ . In the case  $N = 1$  there are two disjoint regions, but for  $N = 2$  there is only one. If there were no temporal feedback (i.e.  $\gamma = 0$ ), then the traveling wave would be unstable. In this example it is not possible

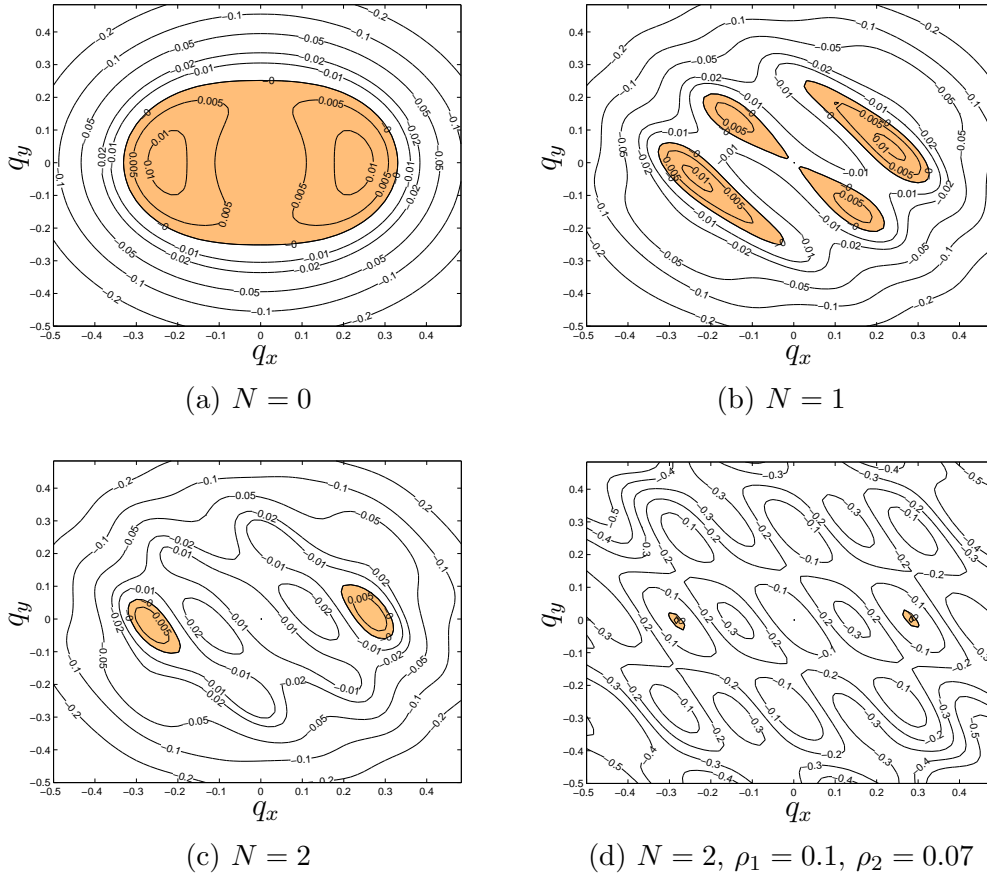


Fig. 4. The figures show contour plots of  $\alpha(\mathbf{q})$  close to  $\mathbf{q} = \mathbf{0}$  in the three cases  $N = 0, 1, 2$ . As  $|\mathbf{q}| \rightarrow \infty$ ,  $\alpha(\mathbf{q}) \rightarrow -\infty$ . Note that  $\alpha(\mathbf{q})$  corresponds to the largest real part of the eigenvalues of the linearized system with no temporal feedback (i.e.  $\gamma = 0$ ). The regions which have positive eigenvalues (corresponding to instabilities) are shaded in. Parameters used are  $b_1 = 2.5$ ,  $b_3 = 2$ , and  $\mathbf{k} = (0.285, 0)$ .  $\Delta \mathbf{x}_1$  is parallel to  $(1, 1)$ ,  $\Delta \mathbf{x}_2$  is parallel to  $\mathbf{k}$ , and  $\Delta \mathbf{x}_j \cdot \mathbf{k} = 2\pi$ . In (a), (b) and (c),  $\rho_1 = 0.01$  and  $\rho_2 = 0.007$ , which are the parameters used in later investigations. In (d)  $\rho_1$  and  $\rho_2$  are increased by a factor of ten, and there are still unstable regions, which cannot be made to vanish no matter how large we choose the  $\rho_j$ . The plots of  $\alpha(\mathbf{q})$  for the other values of  $\mathbf{k}$  used in Section 6 are very similar, and so we do not show them here.

to suppress all the instabilities using just the spatial feedback; figure 4(d) has spatial feedback ten times that of (a)-(c). The  $\mathbf{q}$  which are still unstable are centered around points which satisfy  $\mathbf{q} \cdot \Delta \mathbf{x}_j = 2\pi m$  for some  $m \in \mathbb{N}$ , so the terms proportional to  $\rho_j$  in (10) vanish (i.e. these  $\mathbf{q}$  are unaffected by the spatial feedback). Therefore, however large the  $\rho_i$  are in this example, these  $\mathbf{q}$  will still be unstable. It may, in other examples, be possible that the traveling wave can be stabilized using only spatial feedback. Examples of this for the one-dimensional CGLE are shown in [21]. We now give more details on the addition of temporal feedback to the two cases  $N = 1$  and  $N = 2$ .

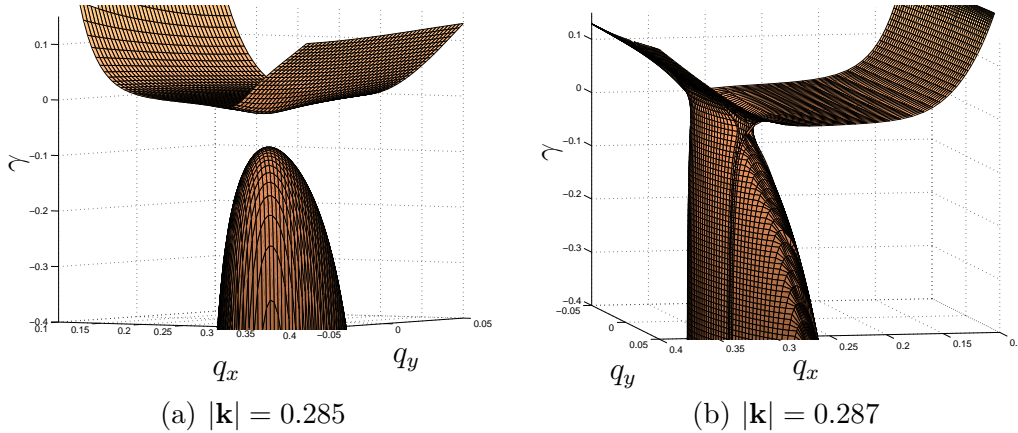


Fig. 5. The two plots show surfaces of Hopf bifurcations for two values of  $|\mathbf{k}|$ . The regions above the upper surface and below the lower surfaces are regions of unstable perturbations. In (a) the surfaces are disjoint and so there is some range of  $\gamma$  for which all perturbations will decay and so the traveling waves can be stabilized. In (b) this is not the case. Notice that the range of  $\mathbf{q}$  in these plots includes that where  $\alpha(\mathbf{q}) > 0$  (see figure 4(c)). Compare also with figure 6, which shows plots of the Floquet multipliers at  $\gamma = -1/\Delta t$ . Parameters used are  $b_1 = 2.5$ ,  $b_3 = 2$ ,  $\rho_1 = 0.01$ ,  $\rho_2 = 0.007$ .  $\Delta\mathbf{x}_1$  is parallel to  $(1, 0)$  and  $\Delta\mathbf{x}_2$  is parallel to  $(1, 1)$ .

### 6.1 $N=2$

Parameters are chosen as described above. We consider two values of  $\mathbf{k}$ ,  $\mathbf{k} = (0.285, 0)$  and  $\mathbf{k} = (0.287, 0)$ . In both cases, the value of  $-1/\Delta t \approx -0.04$ .

Figure 5 shows bifurcation surfaces for the two cases. In the first case, the surfaces are disjoint and so the traveling wave can be stabilized for a range of choices of  $\gamma$ , which include  $-1/\Delta t$ . In the second case, the two surfaces have joined, and there is no choice of  $\gamma$  for which all  $\mathbf{q}$  perturbations are stable.

Figure 6 shows the real part of the Floquet exponents of the linearized system at  $\gamma = -1/\Delta t$ . We can see that for  $|\mathbf{k}| = 0.285$ , the growth rates are negative for all  $\mathbf{q}$ , so the traveling wave is stable. For  $|\mathbf{k}| = 0.287$ , there are two (symmetry-related) regions in the  $\mathbf{q}$ -plane which have positive growth rates and hence the traveling wave is unstable.

### 6.2 $N=1$

We now investigate whether the traveling waves can be stabilized using only one spatially shifted term. We first investigate the same example as used above for  $N = 2$ , but only use the spatial shift  $\Delta\mathbf{x}_1$  which is parallel to the vector  $(1, 1)$ . (Note that we cannot use only the second spatial shift  $\Delta\mathbf{x}_2$  since it is



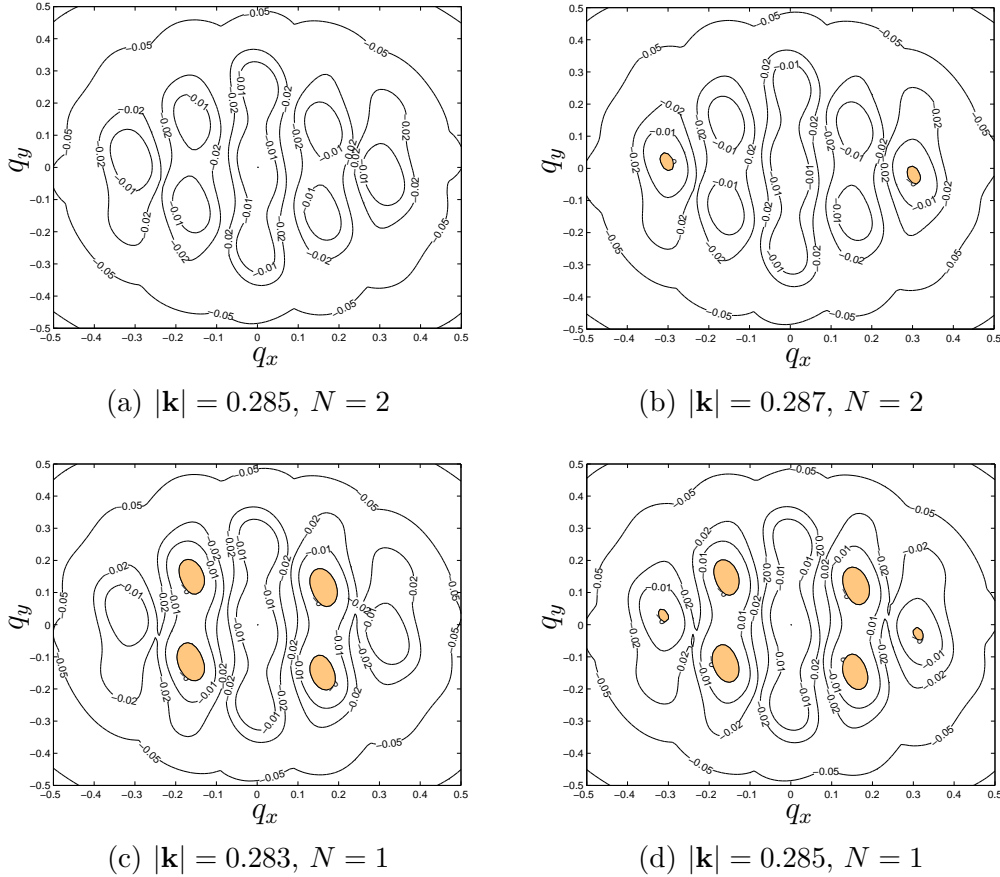


Fig. 6. The contour plots show the real parts of the Floquet exponents of the linearized system at  $\gamma = -1/\Delta t \approx -0.04$ . The upper two plots show  $|\mathbf{k}| = 0.285, 0.287$ ,  $N = 2$ , and the lower two show  $|\mathbf{k}| = 0.283, 0.285$ ,  $N = 1$ . The regions with positive growth rate are shaded in, as in Figure 4. We can see that for  $N = 2$ , the case  $|\mathbf{k}| = 0.285$  is stable but the case  $|\mathbf{k}| = 0.287$  is unstable. For  $N = 1$  there are additional regions of instability so the wave is not stabilized. Parameters used are  $b_1 = 2.5$ ,  $b_3 = 2$ ,  $\rho_1 = 0.01$ ,  $\rho_2 = 0.007$ .  $\Delta \mathbf{x}_1$  is parallel to  $(1, 0)$  and  $\Delta \mathbf{x}_2$  is parallel to  $(1, 1)$ .

parallel to  $\mathbf{k}$ .) Figure 6 shows the real part of the Floquet exponents of the linearized system at  $\gamma = -1/\Delta t$  for this case, for two values of  $|\mathbf{k}|$ . Note that there are more regions of instability in the  $N = 1$  case than the  $N = 2$  case. The instability at  $\mathbf{q} \approx (0.3, 0)$  is present in both cases, and is suppressed as  $|\mathbf{k}|$  is varied. However, in the  $N = 1$  case, there are additional regions of unstable  $\mathbf{q}$  which are not stabilized at these parameter values.

Figure 7 shows the real part of the Floquet exponents for a second parameter set, for which the wave can be stabilized using only one spatially shifted term. In this second example, all parameters are the same except that the spatial shift  $\Delta \mathbf{x}_1$  is parallel to the vector  $(1, 0.2)$ , and  $\rho_1 = 0.1$ . The two plots show the real parts of the exponents of the linearized system with and without the temporal feedback (that is,  $\gamma = 0$  and  $\gamma = -1/\Delta t$ ). There are no positive

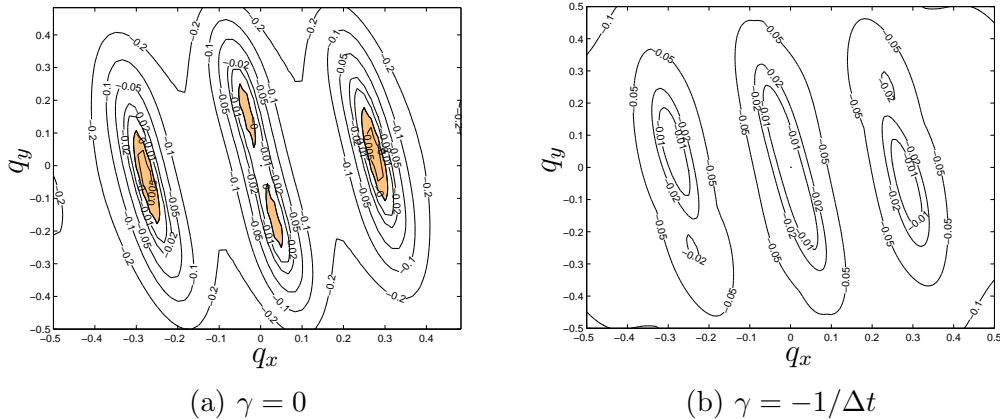


Fig. 7. The two plots show the real part of the Floquet exponents of the linearized system for  $|\mathbf{k}| = 0.284$ , and  $N = 1$ . In 7(a) there is no temporal feedback (i.e.  $\gamma = 0$ ). In 7(b)  $\gamma = -1/\Delta t$ . The regions with positive growth rate are shaded in, as in Figure 4, so we can see that with the temporal feedback, the plane wave is stabilized. Parameters used are  $b_1 = 2.5$ ,  $b_3 = 2$ ,  $\rho_1 = 0.1$ , and  $\Delta \mathbf{x}_1$  is parallel to  $(1, 0.2)$ .

growth rates when  $\gamma = -1/\Delta t$  and hence the traveling wave can be stabilized.

## 7 Discussion

In this paper we have examined the possibility of stabilizing traveling waves of the CGLE in two spatial dimensions using a combination of both temporal and spatial feedback. The feedback is noninvasive, in that it vanishes at the targeted wave solution, and is a generalization of that first proposed by Pyragas [3]. Our analysis is a local linear stability analysis which involves the study of a linear delay equation. The analysis is similar to that in [21], for the 1D CGLE. However, in the 2D case, the spatial shifts  $\Delta \mathbf{x}_j$  must be carefully chosen as otherwise there may be some perturbations  $\mathbf{q}$  which are unaffected by the spatial feedback, meaning the wave cannot be stabilized for any values of the control parameters. We show that if the  $\Delta \mathbf{x}_j$  are correctly chosen, the results of [21] that the ‘best’ value of the gain is  $\gamma = -1/\Delta t$  still holds.

We expect that this method of using noninvasive feedback to stabilize otherwise unstable waves could also be applied to amplitude equations other than the CGLE. One property of the CGLE which simplifies the analysis is that the form of the wave and its dispersion relation can be written down in closed form, and are particularly simple. For other amplitude equations this will not be the case. A lack of knowledge of the dispersion relation means that it is not possible to choose *a priori* the time delay and two spatial shifts in a consistent way so that all temporal and spatial feedback terms vanish simultaneously. It

may be possible, however, to circumvent this difficulty if just one spatial term and one temporal delay term are employed in the feedback; a single wave may then satisfy the criterion that the feedback vanish when it is realized. However, the unknown dispersion relation will then be selecting its direction of travel.

In our analysis, we assumed the feedback parameters  $\gamma$  and  $\rho_j$  were real. This is a mathematically convenient choice since the control matrix then ends up being a multiple of the identity. However, the choice of *real* gain coefficients for the control terms does not seem natural when all other coefficients in the *complex* Ginzburg–Landau equation are complex. Future work on this problem will consider the case of complex gain parameters.

## Acknowledgements

The authors would like to thank Luis Mier y Teran for assistance using DDE-BIFTOOL. This research was supported by NSF grant DMS-0309667.

## References

- [1] M. Golubitsky, I.N. Stewart and D.G. Schaeffer, *Singularities and Groups in Bifurcation Theory: Vol. II*. Appl. Math. Sci. Ser. **69**, Springer-Verlag, New York (1988).
- [2] E. Ott, C. Grebogi, and J. A. Yorke, Controlling Chaos, *Phys. Rev. Letts.*, 1990 **64(11)**, 1196–1199.
- [3] K. Pyragas, Continuous control of chaos by self-controlling feedback, *Phys. Letts. A*, 1992 **170**, 421–428.
- [4] K. Pyragas and A. Tamaševičius, Experimental control of chaos by delayed self-controlling feedback, *Phys. Letts. A*, 1993 **180**, 99.
- [5] D.J. Gauthier, D.W. Sukow, H.M. Concannon and J.E.S. Socolar, Stabilizing unstable periodic orbits in a fast diode resonator using continuous time-delay autosynchronization, *Phys. Rev. E*, 1994 **50**, 2343.
- [6] S. Bielawski, D. Derozier and P. Glorieux, Controlling unstable periodic orbits by a delayed continuous feedback, *Phys. Rev. E*, 1994 **49**, R971.
- [7] Th. Pierre, G. Bonhomme and A. Atipo Controlling the Chaotic Regime of Nonlinear Ionization Waves using the Time-Delay Autosynchronization Method, *Phys. Rev. Lett.*, 1996 **76**, 2290.
- [8] Th. Mausbach, Th. Klinger, A. Piel, A. Atipo, Th. Pierre and G. Bonhomme, Continuous control of ionization wave chaos by spatially derived feedback signals, *Phys. Lett. A*, 1997 **228**, 373.

- [9] T. Fukuyama and H. Shirahama and Y. Kawai, Dynamical control of the chaotic state of the current-driven ion acoustic instability in a laboratory plasma using delayed feedback, *Physics of Plasmas*, 2002 **9**, 4525.
- [10] A. L. Fradkov, R. J. Evans, and B. R. Andrievsky, Control of chaos: methods and applications in mechanics, *Phil. Trans. R. Soc. A*, 2006, **364**, 2279–2307.
- [11] F.W. Schneider, R. Blittersdorf, A. Förster, T.Hauck, D. Lebender and J.Müller, Continuous Control of Chemical Chaos by Time Delayed Feedback, *J. Phys. Chem.*, 1993 **97**, 12244.
- [12] A. Lekebusch, A. Förster and F.W. Schneider, Chaos Control in an Enzymatic Reaction, *J. Phys. Chem.*, 1995 **99**, 681.
- [13] P. Parmananda, R. Madrigal. M. Rivera, L. Nyikos, I.Z. Kiss and V. Gáspár, Stabilization of unstable steady states and periodic orbits in an electrochemical system using delayed-feedback control, *Phys. Rev. E*, 1999 **59**, 5266
- [14] I. Z. Kiss, Z. Kazsu, and V. Gaspar, Tracking unstable steady states and periodic orbits of oscillatroy and chaotic electrochemical systems using delayed feedback control, *Chaos*, 2006, **16**.
- [15] K. Pyragas, Delayed feedback control of chaos, *Phil. Trans. R. Soc. A*, 2006, **364**, 2309–2334.
- [16] J. E. S. Socolar, D. W. Sukow and D. J. Gauthier, Stabilizing unstable periodic orbits in fast dynamical systems *Phys. Rev. E*, 1994, **50(4)**, 3245–3248.
- [17] M.E. Bleich, J.E.S. Socolar, Controlling spatiotemporal dynamics with time-delay feedback *Phys. Rev. E*, 1996, **54(1)**.
- [18] C. Beta, and A. S. Mikhailov, Controlling spatiotemporal chaos in oscillatory reaction-diffusion systems by time-delay autosynchronization, *Physica D*, 2004, **199**, 173–184.
- [19] A. A. Golovin and A. A. Nepomnyashchy, Feedback control of subcritical oscillatory instabilities, *Phys. Rev. E* 2006 **73**.
- [20] S. Boccaletti and J. Bragard, Controlling spatio-temporal chaos in the scenario of the one-dimensional complex Ginzburg–Landau equation, *Phil. Trans. R. Soc. A*, 2006, **364**, 2383–2395.
- [21] K. Montgomery and M. Silber, Feedback Control of Traveling Wave Solutions of the Complex Ginzburg Landau Equation, *Nonlinearity*, 2004, **17(6)**, 2225–2248.
- [22] W. Lu, D. Yu, R. G. Harrison, Control of patterns in spatiotemporal chaos in optics, *Phys. Rev. Letts.*, 1996, **76(18)**, 3316–3319.
- [23] I. Harrington and J.E.S Socolar, Limitation on stabilizing plane waves via time-delay feedback, *Phys. Rev. E*, 2001, **64**.
- [24] O. Diekmann, S. A. van Gils, S. M. Verduyn-Lunel and H. -O. Walther, *Delay Equations, Functional, Complex, and Nonlinear Analysis* Springer, New York, 1995.

- [25] R. D. Driver, *Ordinary and Delay Differential Equations*. Springer–Verlag, New York, 1997.
- [26] H. Nakajima, On analytical properties of delayed feedback control, *Phys. Letts. A*, 1997, **232**, 207–210.
- [27] B. Fiedler, V. Flunkert, M. Georgi, P. Hovel and E.Scholl, Refuting the odd number limitation of time-delayed feedback. *Phys. Rev. Lett.*, 2007, **98**, 114101.
- [28] W. Just, B. Fiedler, M. Georgi, V. Flunkert, P. Hovel and E.Scholl, Beyond the odd number limitation: a bifurcation analysis of time-delayed feedback control. *Preprint*.
- [29] T. Ushio, Limitation of delayed feedback control in nonlinear discrete-time systems. *IEEE Trans. CAS-I*, 1996, **43** 815–816.
- [30] K. Engelborghs, T. Luzyanina and G. Samaey, DDE-BIFTOOL v. 2.00 user manual: a Matlab package for bifurcation analysis of delay differential equations, Technical Report TW-330, Department of Computer Science, K.U.Leuven, Leuven, Belgium, 2001.